A Miniaturized LPF with Sharp Transition-band Using Semi-circle Resonators

Saeed Roshani [1], A. R. Golestanifar [2], A. H. Ghaderi [2], and Sobhan Roshani [1]

[1] Department of Electrical Engineering, Kermanshah Branch, Islamic Azad University, Kermanshah, Iran

[2] Young Researchers and Elite Club, Kermanshah Branch, Islamic Azad University, Kermanshah, Iran

Abstract ─ In this paper, a miniaturized microstrip low-pass filter (LPF) with sharp transition-band, wide stop-band and negligible insertion-loss in pass-band is proposed using semi-circle and butterfly resonators. The cutoff frequency of the proposed LPF is 1.75 GHz. The proposed LPF presents a wide stop-band from 2.1 to 23.73 GHz (2^{nd}-14^{th} harmonics) with -20 dB attenuation level. The overall dimension of the proposed filter is $0.11\lambda_g \times 0.1\lambda_g$. The sharpness of transition-band is 112 dB/GHz, from 1.75 to 2.26 GHz with corresponding attenuation levels of -3 dB and -60 dB, respectively. The insertion-loss in pass-band is less than 0.05 dB. The proposed LPF is simulated, fabricated and measured, which there is a good agreement between the results of simulation and measurement. The LPF has been designed for L-band applications**.**

Index Terms ─ L-band, LPF, open stub, semi-circle resonator, sharp transition-band.

I. INTRODUCTION

Microstrip low-pass filters with small size, low cost, wide stop-band and sharp cut-off frequency are necessary demand for wireless communication circuits to suppress undesirable signals [1, 2]. In [3], a low-pass filter with sharp transition-band was introduced using defected ground structure (DGS). This filter suffers, narrow stop-band and large circuit dimension. In [4], a miniaturized LPF with high return-loss in pass-band was reported using interdigital structure. Slow transition-band and the limited stop-band are draw backs of this work. In [5], a LPF with sharp cut-off frequency was presented using triangular and T-shaped resonators. This structure has low suppression level in stop-band and occupied large area. In [6], a microstrip LPF with stepped-impedance units was presented. Negligible ripple in pass-band and small size are advantages of this work, although roll-off rate is not so sharp. A low-pass filter was reported in [7], which has low suppression level in the stop-band area. In [8], a LPF with hairpin-resonator was presented, which the stop-band is narrow. In [9, 10], LPFs with small size were introduced using hairpin resonators, which gradual transition-band and narrow stop-band are undesired features of these works. In [11], a low-pass filter with defected rectangular resonator was reported. The cut-off frequency of the filter is not sharp and the stopband is narrow. In [12], a LPF with low rejection level and narrow stop-band was introduced. In [13], a microstrip LPF was reported using multi-mode resonators, which the transition-band is not sharp. In [14], a LPF with wide stop-band was presented based on DGS. The transition-band of this filter is not so sharp. In [15], a LPF with Butterworth response was presented. This LPF has a sharp transition-band and wide stop-band, but the structure has low attenuation level compared with conventional Butterworth filter. In [16], a microstrip structure with rectangular resonators was reported. To extend the stop-band, a DGS composed of four u-shaped resonators was utilized. However, the presented LPF suffers, ripple in pass-band and slow transition-band.

In this study, a novel structure with sharp transition–band, wide stop-band, low ripple in passband and miniaturized size is proposed. The stop-band is extended to 23.73 GHz with -20 dB attenuation level. All electro-magnetic (EM) simulations of microstrip layouts and all L-C simulations of equivalent circuits are performed using Advanced Design System (ADS 2011.10) software (Agilent Technologies, Santa Clara, CA). Scattering parameters measurement of fabricated device and EM simulations results of proposed LPF are in good agreement, which confirms the validity of the proposed LPF.

II. DESIGN PROCESS

A. Primitive semi-circle resonator

The primitive semi-circle resonator is designed on RT/Duroid 5880 substrate with relative permittivity of 2.2, thickness of 0.381 mm and loss-tangent of 0.0009. Also copper with thickness of 10μm is utilized as conductor strip lines. In order to design an LPF with wide stopband, a semi-circle resonator is used. The

Submitted On: October 14, 2016
Accepted On: March 19, 2017

layout of the primitive semi-circle resonator is depicted in Fig. 1 (a). This structure consists of a high-impedance line and a semi-circle shaped stub, which they are connected to the transmission line, based on Fig. 1 (a). The L-C equivalent circuit of this resonator is demonstrated in Fig. 1 (b), which, the inductances and capacitance of the corresponding transmission lines are L_1, L_2 and C_1, respectively. L_3 is inductance of high-impedance line and C_2 is the sum of open-ended and low-impedance lines capacitances. The EM simulations and L-C equivalent circuit simulation results are in good agreement and there is a transmission-zero (T_{Z1}) at 8.8 GHz with -55 dB attenuation level as shown in Fig. 1 (c). The L-C equivalent circuit values are optimized by ADS software and they are summarized in Table 1. The dimensions of this structure are: A_1=9.73, A_2=3.96, A_3=0.23, A_4=0.1, A_5=1.17, A_6=1.5, r=4.12 (unit: millimeter) and ϕ_1=170°.

Table 1: The optimized values of L-C equivalent circuit

Parameter	C_1	C_2	L_1	L_2	L_3
Values	1.264	0.561	7	2.74	0.597

(Units: C=[pF]; L=[nH]).

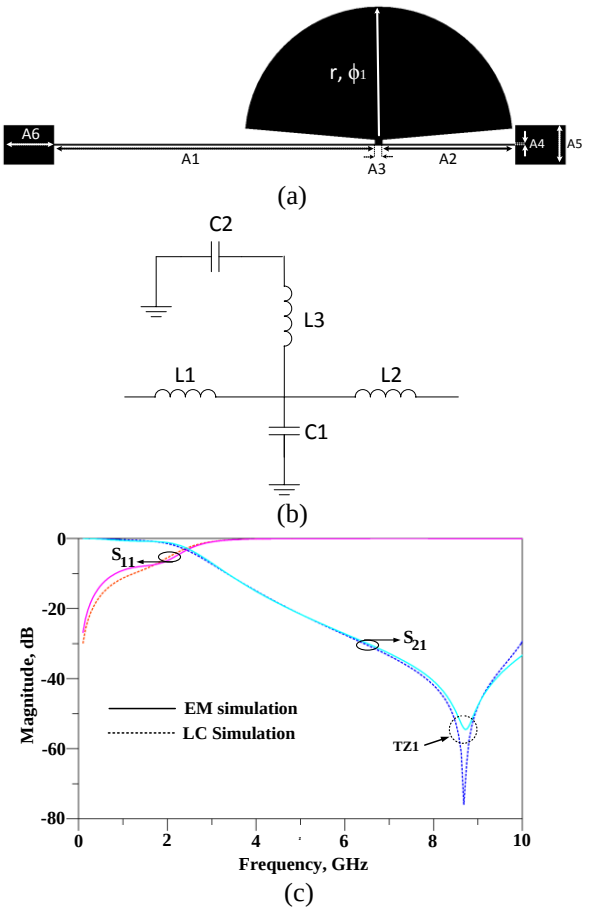

Fig. 1. (a) Layout, (b) L-C equivalent circuit, and (c) EM and L-C simulations of primitive semi-circle resonator.

In order to have a focus on computational theory, the applied resonators are modeled using LC equivalent circuits. To find accurate using LC equivalent circuits, applied microstrip discontinuities and components that are encountered in the proposed filter designs are described in Fig. 2. In the layout of proposed filter steps, open-ends, high-impedance short-line element and low-impedance short-line element are used, which these components and LC equivalent circuits are shown in Fig. 2. For a symmetrical step, the capacitance and inductances of the equivalent circuit indicated in Fig. 2 (a). At the open end of a microstrip line the fields do not stop abruptly but extend slightly further due to the effect of the fringing field. This effect can be modeled either with an equivalent shunt capacitance as shown in Fig. 2 (b). In Fig. 2 (c), a short length of high-impedance line terminated at both ends by low impedance is represented by a π-equivalent circuit. For the dual case shown in Fig. 2 (d), a short length of low-impedance line terminated at either end by high impedance is represented by a T-equivalent circuit.

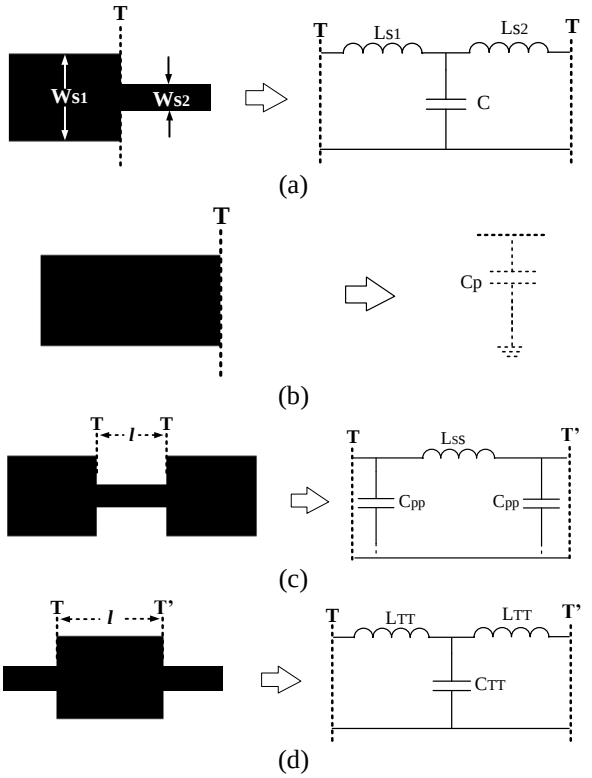

Fig. 2. Microstrip discontinuities: (a) step, (b) open-end, (c) high-impedance short-line, and (d) low-impedance short-line elements and their equivalent circuits [2].

The ABCD-parameters for a two-port network are [1]:

$$\begin{bmatrix} V_1 \\ I_1 \end{bmatrix} = \begin{bmatrix} A & B \\ C & D \end{bmatrix} \begin{bmatrix} V_2 \\ I_2 \end{bmatrix}. \quad (1)$$

According to (1), the ABCD-parameters of L-C equivalent circuit for primitive semi-circle resonator are obtained as follows:

$$A = C_1L_1S^2 + \frac{C_2L_1S^2}{C_2L_3S^2+1} + 1, \quad (2)$$

$$B = L_1S + C_1L_1L_2S^3 + \frac{C_2L_1L_2S^3}{C_2L_3S^2+1} + L_2S\ ), \quad (3)$$

$$C = C_1S + \frac{C_2S}{C_2L_3S^2+1}, \quad (4)$$

$$D = C_1L_2S^2 + \frac{C_2L_2S^2}{C_2L_3S^2+1} + 1. \quad (5)$$

The S-parameter (S_{21}) in terms of ABCD-parameters is [1]:

$$S_{21} = \frac{2}{A+B/Z_0+CZ_0+D}. \quad (6)$$

From (6), S_{21} of L-C equivalent circuit is:

$$S_{21} = \left(2Z_0(C_2L_3S^2+1)\right)/(S^5(C_1L_1C_2L_2L_3) + S^4(C_1L_1C_2L_3Z_0 + C_1L_2C_2L_3Z_0) + S^3\left(C_1L_3C_2{Z_0}^2 + C_2L_1L_3 + C_1L_1L_2 + C_2L_3L_2\right) + S^2(C_1L_1Z_0 + C_1L_2Z_0 + C_2L_2Z_0 + C_2L_1Z_0 + 2C_2L_3Z_0) + S\left(C_1{Z_0}^2 + C_2{Z_0}^2 + L_1 + L_2\right) + 2Z_0 + 1). \quad (7)$$

The T_{Z1} is obtained using Equation (7):

$$F_{z1} = \frac{1}{2\pi\sqrt{C_2L_3}}. \quad (8)$$

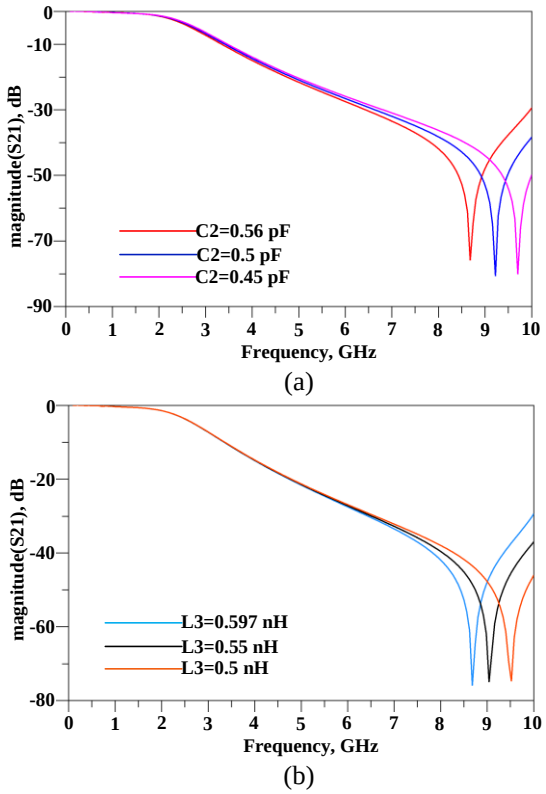

Fig. 3. (a) Variations of Fz1 as a function of C2, and (b) variations of Fz1 as a function of L3.

According to (8), the location of T_{Z1} is a function of C_2 and L_3. According to Fig. 3 (a) and Table 1, decreasing in value of C_2 (when L_3 is unchanged) moves T_{Z1} to the higher frequencies and vice versa. Also, decreasing in value of L_3 (when C_2 is unchanged) moves T_{Z1} to the higher frequencies and vice versa, as shown in Fig. 3 (b). So, the values of L-C equivalent circuit in Table 1 is selected, to achieve a transmission-zero at the desired frequency.

B. Symmetrical semi-circle resonator

To achieve a wide stop-band and better performance, symmetrical semi-circle resonator is designed. The substrate and conductor material are same as mentioned below. The layout of the symmetrical semi-circle resonator is depicted in Fig. 4 (a). According to Fig. 4 (b), this resonator with simple structure can generate a wide stop-band (from 3.9 to 22 GHz with -20 dB attenuation level). Although the transition-band is not very sharp. The proposed structure creates a transmission-zero (T_{Z2}) at 13.8 GHz with -47 dB attenuation, as seen in Fig. 4 (b).

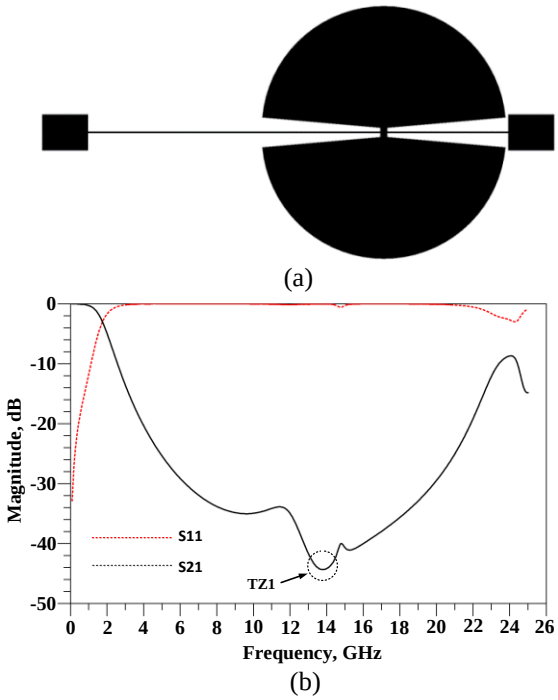

Fig. 4. (a) Layout and (b) EM simulation results of symmetrical semi-circle resonator.

C. Butterfly resonator

To achieve a sharp transition-band, a butterfly resonator is proposed. The layout and L-C equivalent circuit of butterfly resonator are demonstrated in Fig. 5 (a) and 5 (b), respectively. According to Fig. 5 (b), the corresponding inductances and capacitance of transmission line are L_4, L_5 and C_3, respectively. L_6 and L_7 are the inductances of high-impedance line and low impedance stub, respectively. C_4 is the sum of open stub and low-impedance stub capacitances. According to Fig.

5 (c), the EM simulations and L-C equivalent circuit simulation results are in good agreement. Also there is a transmission-zero (T_{Z3}) at 2.4 GHz with -52 dB attenuation level as seen in Fig. 5 (c). The L-C equivalent circuit values are optimized by ADS software and they are summarized in Table 2. The dimensions of this resonator are: A_7=10.45, A_8=3.07, A_9=5.5, A_{10}=0.4, A_{11}=3.92, A_{12}=0.15 (unit: millimeter) and ϕ_2=90°. The substrate and conductor material are same as mentioned below.

Table 2: The optimized values of L-C equivalent circuit

Parameter	L_4	L_5	L_6	L_7	C_3	C_4
Values	3.24	7.415	2.364	0.66	0.422	0.819

(Units: C=[pF]; L=[nH]).

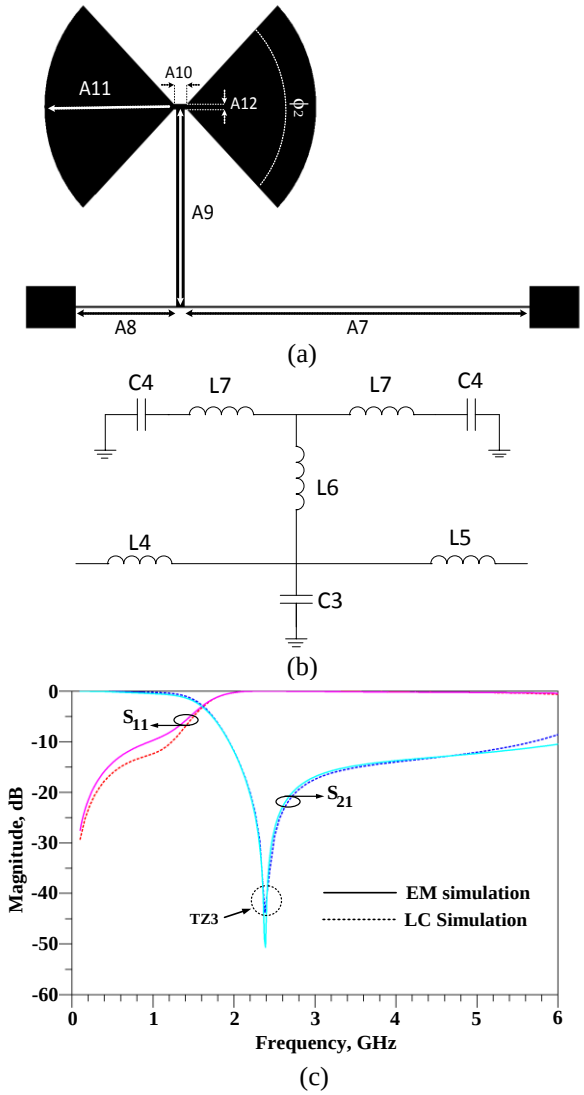

Fig. 5. (a) Layout, (b) L-C equivalent circuit, and (c) EM and L-C simulations of butterfly resonator.

As the simulation results shown in the Fig. 5 (c), the butterfly resonator has good performance. The insertion loss in pass band is zero (S_{12}= S_{21}= 0 dB). In the stop band this resonator creates a strong transmission-zero (T_{Z3}) near the desired cut-frequency of the proposed LPF, which results in a good performance compare to the primitive resonator. Unfortunately, the input and output return losses (S_{11}, S_{22}) of butterfly resonator in pass band are not so good and the transition band is not so sharp, therefore to improve the performance symmetrical semi-circle resonator and butterfly resonator are combined together, which will be discussed in Section II.D

The ABCD-parameters of L-C equivalent circuit for butterfly resonator are as follows:

$$A = C_3L_4S^2 + \frac{2C_4L_4S^2}{(2C_4L_6+C_4L_7)S^2+1} + 1, \quad (9)$$

$$B = L_4S + C_3L_4L_5S^3 + \frac{2C_4L_4L_5S^3}{(2C_4L_6+C_4L_7)S^2+1} + L_5S, \quad (10)$$

$$C = C_3S + \frac{2C_4S}{(2C_4L_6+C_4L_7)S^2+1}, \quad (11)$$

$$D = C_3L_5S^2 + \frac{2C_4L_5S^2}{(2C_4L_6+C_4L_7)S^2+1} + 1. \quad (12)$$

From (6), S_{21} of L-C equivalent circuit for butterfly resonator is:

$$S_{21} = \frac{\left(2Z_0\left((2C_4L_6+C_4L_7)S^2+1\right)\right)}{(S^5(2C_4L_6L_5C_3L_4+L_5C_3C_4L_4L_7)} + S^4(2Z_0C_4L_6C_3L_4 + Z_0C_3L_4C_4L_7 + 2Z_0L_5C_3C_4L_6 + Z_0L_5C_3C_4L_7) + S^3\left(2{Z_0}^2C_3C_4L_6 + {Z_0}^2C_3C_4L_7 + 2L_4C_4L_6 + L_4C_4L_7 + L_5C_3L_4 + 2L_5C_4L_6 + L_5C_4L_7\right) + S^2(C_3L_5Z_0 + 2C_4L_5Z_0 + 2Z_0C_4L_4 + 4Z_0C_4L_6 + 2Z_0C_4L_7 + Z_0C_3L_4) + S\left(C_3{Z_0}^2 + 2C_4{Z_0}^2 + L_4 + L_5\right) + 2Z_0 + 1). \quad (13)$$

The T_{Z3} is obtained using Equation (13):

$$F_{z3} = \frac{1}{2\pi\sqrt{(2C_4L_6+C_4L_7)}}. \quad (14)$$

According to (14), the location of T_{Z3} is a function of L_6 and C_4, which L_6 and C_4 are inductance and capacitance of A_9 and A_{11} in Fig. 5 (a), respectively. Decreasing in the value of A_9 (when A_{11} is unchanged) and decreasing in the value of A_{11} (when A_9 is unchanged), moves T_{Z3} to the higher frequencies, as depicted in Fig. 6 (a) and 5 (b), respectively. So to have sharp transition-band, T_{Z3} is tuned at 2.4 GHz and values of L-C equivalent circuit are obtained in Table 2.

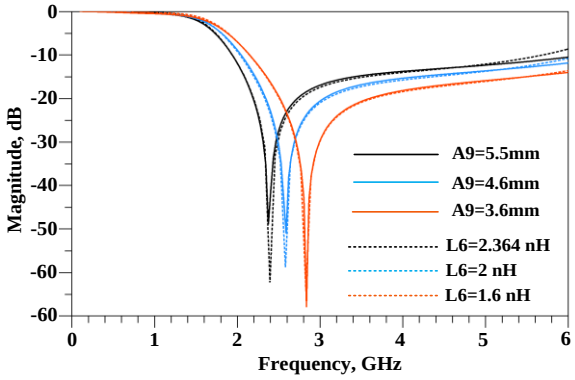

(a)

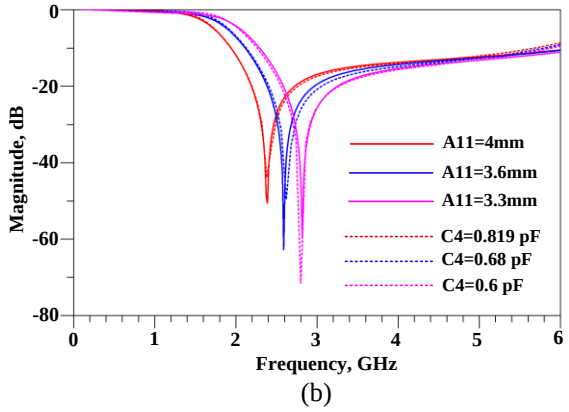

(b)

Fig. 6. (a) Variations of Fz_3 as a function of L_6 and A_9, and (b) variations of Fz_3 as a function of C_4 and A_{11}.

D. Primitive LPF

To approach a wide stop-band and sharp transition-band, symmetrical semi-circle resonator and butterfly resonator are combined, with same substrate and conductor strip line material as mentioned below, based on Fig. 7 (a). Although this structure, suffers from high ripple in pass-band and low return-loss in pass-band and a transmission pole that limits the suppression level and stopband bandwidth of primitive low pass filter, as seen in Fig. 7 (b). The distance between the resonators is A_{13}=6.26 mm.

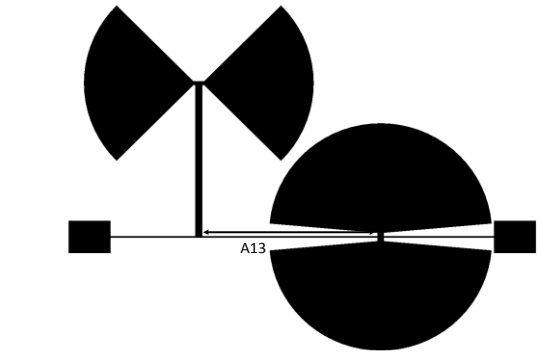

(a)

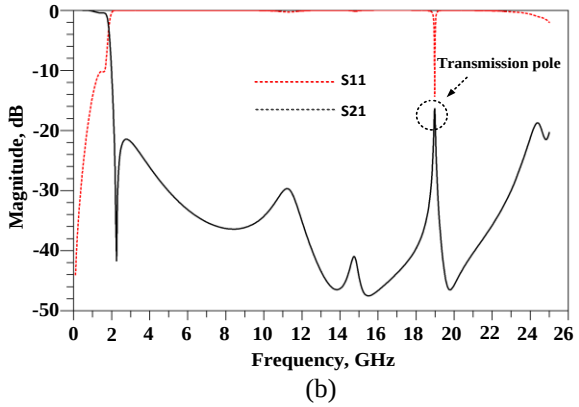

(b)

Fig. 7. (a) Layout and (b) EM simulations of primitive LPF.

E. Proposed LPF

According to Fig. 7 (b), there is a transmission-pole at 19 GHz, which limits the stop-band of primitive LPF. Therefore, two suppressing cells, with same substrate and conductor material as mentioned below, are added to primitive LPF to extend the stop-band and the transmission line is bended without increasing dimension as depicted in Fig. 8 (a). EM simulations illustrate wide stop-band, sharp transition-band. Moreover, the ripple in pass-band has been reduced (less than 0.05 dB) and a good return-loss in pass-band (20 dB) is achieved, as seen in Fig. 8 (b). Physical dimensions of the proposed LPF are: L_1=4.33, L_2=3.96, L_3=1.8, L_4=1, L_5=1.5, L_6=1.17, L_7=3.07, L_8=0.96, L_9=1.22, L_{10}=0.97, L_{11}=5.5, L_{12}=0.8, D_1=0.4, D_2=0.15, D_3=0.23, D_4=0.05, D_5=0.3, D_6=0.1, R_1=0.5, R_2=3.92 and R_3=4.12 (all in millimeters). Also θ_1=90˚, θ_2=170˚.

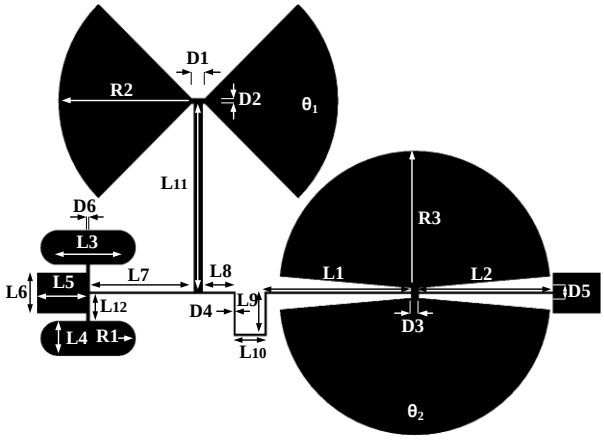

(a)

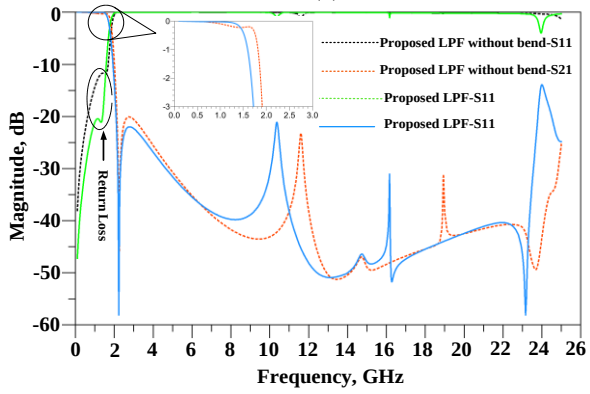

(b)

Fig. 8. (a) Layout and (b) EM simulations of proposed LPF.

III. MEASURED AND SIMULATED RESULTS

The proposed low-pass filter has been designed and fabricated on the RT-Duorid 5880 substrate with relative permittivity of 2.2, thickness of 0.381 mm and loss-tangent of 0.0009 Also, copper with thickness of 10μm

is utilized as conductor strip lines. The photograph of fabricated low-pass filter is illustrated in Fig. 9 (a). There is a good agreement between measurement and simulation results, as demonstrated in Fig. 9 (b). The S-parameters are measured using the network analyzer N5230A and. The results demonstrate that, proposed LPF presents very good size reduction compared with previous works.The final circuit dimensions of the proposed low-pass filter are only 13.72 × 12.6 mm^2 ($0.11\lambda_g \times 0.1\lambda_g$). The proposed LPF indicates high suppression in a wide stop-band from 2.1 to 23.73 GHz with more than -20 dB attenuation level (measurement results), which suppresses the 2nd-14th harmonics. The performance comparison among published filters and proposed one have been illustrated in Table 3.

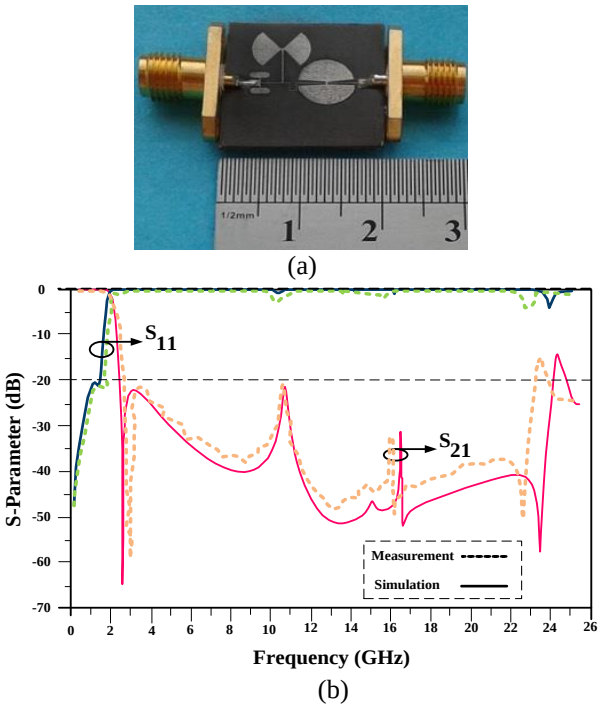

Fig. 9. (a) Photograph of proposed LPF, and (b) EM simulations and measured results

Table 3: Performance comparison among previous filters and proposed one

Refs.	ξ	RSB	SF	NCS	AF	FOM
[3]	95.5	1.359	2	0.540×0.480	2	500.7
[6]	52.8	1.529	2	0.081×0.113	1	17640
[7]	43.9	1.636	1	0.101×0.150	1	4723
[8]	95	1.4	2	0.022	1	12090
[13]	-	1.58	1.5	0.090×0.110	1	-
[14]	78	1.7	2	0.160×0.100	2	8287.5
[16]	129	1.62	2	0.730×0.130	1	4430.8
This work	112	1.674	2	0.110×0.100	1	34088

In Table 3, the sharpness of transition-band (ξ) is:

$$\xi = \frac{\alpha_{max} - \alpha_{min}}{f_s - f_c} \quad (dB/GHz), \tag{15}$$

and α_{max} is -60 dB suppression level; α_{min} is -3 dB suppression level; f_C is the frequency corresponds with -60 dB suppression level and f_c is the corresponding frequency with -3 dB suppression level. The relative stop-band band-width (RSB) is given by:

$$RSB = \frac{stopband\ bandwidth}{stopband\ center\ frequency}. \tag{16}$$

The suppressing factor (SF) is:

$$SF = \frac{suppression\ level}{10}. \tag{17}$$

The normalized circuit size (NCS) is:

$$NCS = \frac{physical\ size\ (length \times width)}{\lambda_g^2}. \tag{18}$$

The λ_g is the length of guided wavelength at -3 dB cut off frequency and for calculation of architecture facture, this parameter has below values: for circuits with 1 dimension is defined 1 and for circuits with three dimension the AF is defined 2.

Finally, the figure of merit (FOM) is defined as:

$$FOM = \frac{RSB \times \xi \times SF}{AF \times NCS}. \tag{19}$$

IV. CONCLUSION

A miniaturized low-pass filter with high FOM and ultra-wide stop-band is proposed. The proposed filter demonstrates very good performance such as low insertion-loss in pass-band, wide stop-band, sharp transition-band and small dimension. The final circuit dimension is only $0.11\lambda g \times 0.1\lambda g$. The cut off frequency of the proposed LPF is 1.75 GHz. The proposed structure suppresses 2nd to 14th harmonics with more than 20 dB attention level. With the above desirable features, the proposed filter is suitable for L-band applications.

ACKNOWLEDGMENT

The authors would like to thank the Kermanshah Branch, Islamic Azad University for the financial support of this research project.

REFERENCES

[1] D. M. Pozar, *Microwave Engineering*. John Wiley & Sons, New York, 2005.

[2] J. S. Hong and M. J. Lancaster, *Microstrip Filters for RF/Microwave Applications*. John Wiley & Sons, New York, 2001.

[3] Y. Zhang, L. Jin, and L. Li, "Design of LPF using Hi-Lo interdigital DGS slot," *IEICE Electronics Express*, vol. 13, no. 9, pp. 1-6, 2016.

[4] L. Li, Z. F. Li, and J. F. Mao, "Compact lowpass filters with sharp and expanded stopband using stepped impedance hairpin units," *IEEE Microwave and Wireless Components Letters*, vol. 20, no. 6, pp. 310-312, 2010.

[5] J. P. Wang, L. Ge, Y. X. Guo, and W. Wu,

"Miniaturised microstrip lowpass filter with broad stopband and sharp roll-off," *Electronics Letters*, vol. 46, no. 8, pp. 573-575, 2010.

[6] L. Shuai, J. Xu, and Z. Xu, "Compact lowpass filter with wide stopband using stepped impedance hairpin units," *Electronics Letters*, vol. 51, no. 1, pp. 67-69, 2014.

[7] F. Wei, L. Chen, and X. W. Shi, "Compact lowpass filter based on coupled-line hairpin unit," *Electronics Letters*, vol. 48, no. 7, pp. 379-381, 2012.

[8] V. Velidi and S. Sanyal, "Sharp roll-off lowpass filter with wide stopband using stub-loaded coupled-line hairpin unit," *IEEE Microwave and Wireless Components Letters*, vol. 21, no. 6, pp. 301-303, 2011.

[9] F. Wei, L. Chen, X. W. Shi, Q. L. Huang, and X. H. Wang, "Compact lowpass filter with wide stopband using coupled-line hairpin unit," *Electronics Letters*, vol. 46, no. 1, pp. 88-90, 2010.

[10] X. B. Wei, P. Wang, M. Q. Liu, and Y. Shi, "Compact wide-stopband lowpass filter using stepped impedance hairpin resonator with radial stubs," *Electronics Letters*, vol. 47, no. 15, pp. 862-863, 2011.

[11] M. Rezaei Khezelia, M. Hayati, and A. Lotfi, "Compact wide stopband lowpass filter using spiral loaded tapered compact microstrip resonator cell," *International Journal of Electronics*, vol. 101, no. 3, pp. 375-382, 2012.

[12] C. J. Chen, "Design of artificial transmission line and low-pass filter based on aperiodic stubs on a microstrip line," *IEEE Transaction on Components, Packing and Manufacturing Technology*, vol. 4, no. 5, pp. 922-928, 2014.

[13] Q. Li, Y. Zhang, and Y. Fan, "Compact ultra-wide stopband low pass filter using multimode resonators," *Electronics Letters*, vol. 51, no. 14, pp. 1084-1085, 2015.

[14] F. C. Chen, H. T. Hu, J. M. Qiu, and Q. X. Chu, "High-selectivity low-pass filters with ultrawide stopband based on defected ground structures," *IEEE Transaction on Components, Packing and Manufacturing Technology*, vol. 5, no. 9, pp. 1313-1319, 2015.

[15] A. K. Verma, N. P. Chaudhari, and A. Kumar, "High performance microstrip transverse resonance lowpass filter," *Microwave and Optical Technology Letters*, vol. 55, no. 5, pp. 1149-1152, 2013.

[16] P. Zhang, M. Li, and J. Wang, "Miniaturized lowpass filter with ultra-wide stopband using dual-plan defected structures," *IEICE Electronics Express*, vol. 12, no. 2, pp. 1-7, 2014.

Saeed Roshani received the B.Sc. degree in Electrical Engineering from Razi University, Kermanshah, Iran in 2008, M.Sc. degree in Electrical Engineering from Shahed University, Tehran, Iran in 2011 and Ph.D. in Electrical Engineering from Razi University in 2015. He performed opportunity research program in Amirkabir University of Technology (Tehran Polytechnics) Iran, in 2014-2015. He graduated as the Best Student of his country among all students of Iran in 2015 and awarded by the First Vice President and Science, Research & Technology Minister. He is currently an Assistant Professor in the Department of Electrical Engineering at Islamic Azad University, Kermanshah, Iran. He has published more than 40 papers in ISI Journals and Conferences and two books. His research interest includes the microwave and millimeter wave devices and circuits, low-power and low-size integrated circuit design.

Alireza Golestanifar was born in Kermanshah, Iran in 1993. He received his B.Sc. degree in Electronics Engineering in 2015 from Islamic Azad University, Kermanshah, Iran and he is now pursuing his M.Sc. degree from Islamic Azad University, Kermanshah, Iran. His current research includes microwave passive circuits and RF integrated circuit design.

Amirhossein Ghaderi was born in Kermanshah, Iran in 1992. He received his B.Sc. degree in Electronics Engineering in 2015 from Islamic Azad University, Kermanshah, Iran (Honor) and he is currently working towards the M.Sc. degree in Electronics Engineering from Islamic Azad University, Kermanshah, Iran. He was selected as the Best Student in the Electronics Engineering Department

and awarded by the University President of Islamic Azad University, Kermanshah, Iran in 2014. His current research includes microwave passive circuits and RF integrated circuit design.

Sobhan Roshani received the B.Sc. degree in Electrical Engineering from Razi University, Kermanshah, Iran in 2010, M.Sc. degree in Electrical Engineering from Iran University of Science & Technology-IUST, Tehran, Iran in 2012 and Ph.D. in Electrical Engineering from Razi University in 2016. His research interest includes switching power amplifiers, microwave circuits, image processing, optimization and neural networks. He is currently working with Department of Electrical Engineering at Islamic Azad University, Kermanshah, Iran.